Substitutional disorder and the optical spectroscopy of gallogermanate crystals

1996 J. Phys.: Condens. Matter 8 3933

(http://iopscience.iop.org/0953-8984/8/21/018)

J. Phys.: Condens. Matter **8** (1996) 3933–3946. Printed in the UK

Substitutional disorder and the optical spectroscopy of gallogermanate crystals

Peter I Macfarlane†, Brian Henderson†, Keith Holliday† and Marek Grinberg‡

† Department of Physics and Applied Physics, University of Strathclyde, Glasgow G1 1XN, UK
‡ Institute of Physics, Nicolas Copernicus University, 87-100 Torun, Poland

Received 6 February 1996

Abstract. Results of optical absorption, photoluminescence, fluorescence lifetime and fluorescence-line-narrowing studies on several Cr^{3+}-doped crystals with the gallogermanate crystal structure are presented. Such crystals are unusual in that most fluoresce via both the broad-band $^4T_2 \rightarrow {}^4A_2$ transition and the sharper $^2E \rightarrow {}^4A_2$ transition (R line), both of which are considerably broadened by the effects of substitutional disorder. An established adiabatic model is used to reproduce the selectively excited broad-band photoluminescence spectra and this shows that the substitutional disorder creates a distribution in the strength of both the octahedral crystal field and the electron–phonon coupling. The variations in electron–phonon coupling are attributed to variations in the strength of the non-octahedral crystal fields that determine the magnitudes of the coupling to non-symmetric phonon modes. This effect is shown to dominate the broadening of the band. The analysis of results of fluorescence-line-narrowing measurements on the R lines shows that these lines are also broadened by a distribution of both octahedral and non-octahedral crystal fields. In the case of crystals that contain a substitutionally disordered site in the close vicinity of the Cr^{3+} ion, the strong-field sites that give rise to R-line emission are shown to comprise an independent distribution and the broadening is dominated by the effects of the non-octahedral component of the crystal field. When the substitutionally disordered sites are further from the Cr^{3+} ion, the broad-band and R-line fluorescence derive from a single distribution of crystal fields. In this case the effect of the variation of the crystal field is again shown to be dominated by the non-octahedral contribution though the R-line fluorescence shows little evidence of this due to the strong-field sites being the extreme of the overall distribution.

1. Introduction

There is considerable interest in the development of laser systems that operate at different wavelengths from those of established technology. The suitability of the Cr^{3+} ion as the optical centre in tunable solid-state lasers led to much research on new hosts for this ion. Shifting the broad-band Cr^{3+} photoluminescence to higher energies is confounded by the crossover into sharp-line luminescence for ions in strong crystal fields. Nevertheless there is scope for extending the tuning range of Cr^{3+} lasers further into the near infra-red by substituting Cr^{3+} ions in hosts having either weaker crystal fields or such strong electron–phonon coupling that the photoluminescence is shifted to much lower energies than the static crystal-field model would imply. The family of Cr^{3+}-doped gallogermanate crystals is characterized by very broad luminescence bands and appeared to offer tuning ranges significantly different to those for Cr^{3+} ions in other hosts. Unfortunately, poor efficiencies and high thresholds make them unsuccessful as laser gain media. Despite this, there is

0953-8984/96/213933+14$19.50

scientific interest in that these are substitutionally disordered crystals in which there is strong inhomogeneous broadening of optical transitions [1], comparable with that in glasses [2–4]. An understanding of the broadening processes in these materials will aid the development of gain media that may be designed to have similarly large tuning ranges without the difficulties that gallogermanates experience.

The purpose of the present paper is to investigate the influence of the distance between the optically active ion and the substitutionally disordered sites. To this end, the optical properties of two Cr^{3+}-doped members of the gallogermanate family, $La_3GaGe_4O_{14}$ (LGGO) and $La_3Ga_5SiO_{14}$ (LGS), are compared with those of two previously reported, $Sr_3Ga_2Ge_4O_{14}$ (SGGO) and $Ca_3Ga_2Ge_4O_{14}$ (CGGO) [1, 5]. In the case of CGGO and SGGO the disordered sites are nearest cation neighbours whereas in LGGO and LGS the disordered sites are further removed. Of particular importance to this study is the determination of the mechanisms that cause the inhomogeneous broadening of the optical transitions and this is achieved through the analysis of the results of absorption, fluorescence-line narrowing, selective excitation and fluorescence lifetime measurements.

Table 1. The site occupation of the gallogermanates.

Crystal	3e sites (cube)	1a site (octahedral)	2d sites (tetrahedral)	3f sites (tetrahedral)	2d sites	$6g_1$ sites	$6g_2$ sites
CGGO	Ca^{2+}	0.5 Ga^{3+} + 0.5 Ge^{4+}	Ge^{4+}	1.5 Ga^{3+} + 1.5 Ge^{4+}	O^{2-}	O^{2-}	O^{2-}
SGGO	Sr^{2+}	0.4 Ga^{3+} + 0.6 Ge^{4+}	Ge^{4+}	1.6 Ga^{3+} + 1.4 Ge^{4+}	O^{2-}	O^{2-}	O^{2-}
LGGO	La^{3+}	Ga^{3+}	Ga^{3+} + Ge^{4+}	Ga^{3+}	O^{2-}	O^{2-}	O^{2-}
LGS	La^{3+}	Ga^{3+}	Ga^{3+} + Si^{4+}	Ga^{3+}	O^{2-}	O^{2-}	O^{2-}

The gallogermanate crystals were first grown in 1980 by Mill and colleagues, and the crystal structure of calcium gallogermanate determined by x-ray diffraction [6–8]. The aspects of the crystal structure most salient to this study are the proximity of the substitutionally disordered sites to the Cr^{3+} ions. The Cr^{3+} ion substitutes at a 1a site, surrounded by a trigonally distorted octahedron of oxygen ions. The nearest cation shell is the 3f site which is substitutionally disordered in CGGO and SGGO but contains only Ga^{3+} ions in LGGO and LGS. The same applies to the next-nearest cation site which is the 1a octahedral site. Finally, the 2d site is furthest removed from the Cr^{3+} site. This site contains Ge^{4+} ions in CGGO and SGGO but is substitutionally disordered in LGGO and LGS. The occupations of all sites for the crystals used in the present study are listed in table 1.

2. Experimental details

The experiments were carried out using crystals of CGGO, SGGO, LGGO and LGS doped with 0.5 at.% Cr^{3+}. The samples were cut and polished to dimensions of $6 \times 3 \times 3$ mm^3 with the long dimension parallel to the *c*-axis of the crystal. Absorption measurements were made at 77 K or 300 K over the range 7500–35 000 cm^{-1} using an Aviv–Cary 14 spectrophotometer. Photoluminescence and photoluminescence lifetime measurements were made by exciting with an Ar^+ laser or an Ar^+-laser-pumped rhodamine 6G tunable dye

laser. The photoluminescence samples were cooled to temperatures in the range 14–300 K by attachment to the cold finger of a cryorefrigerator equipped with optical access for both exciting and emitted radiation. The radiation emitted in a direction parallel to the exciting light was dispersed in a 0.5 m monochromator and detected photoelectrically with either a photomultiplier tube (Hamamatsu R928) or a liquid-nitrogen-cooled Ge detector (North Coast Optics), with lock-in amplifier.

Fluorescence-line-narrowing (FLN) studies used the highly monochromatic output of a Ti–sapphire laser tuned to excite the R lines resonantly. The excitation wavelength was recorded using a wavemeter. The emitted light was dispersed in a 1 m monochromator and detected by a cooled phototube connected to a photon-counting system. The photoluminescence signal was isolated from laser scatter by chopping the laser and gating the photon counter.

3. Experimental results and discussion

3.1. General characteristics of optical spectra

The optical absorption spectra of CGGO, SGGO, LGS and LGGO were measured at 77 K. Both SGGO and CGGO exhibit the usual characteristic of Cr^{3+} ions situated in approximately octahedral crystal fields, namely two broad absorption bands corresponding to transitions from the $^4A_2$ ground state to the $^4T_2$ and $^4T_1$ excited states. The CGGO and SGGO samples also have absorption bands near 20 000, 18 200, 13 300 and 8000 cm^{-1} which are due to Cr^{4+} ions occupying tetrahedral sites [5]. In contrast, LGS and LGGO samples have an intense absorption band near 22 200 cm^{-1} and a much weaker band at longer wavelengths. In LGS the 22 200 cm^{-1} band may be removed by annealing the crystal in H_2 at 1275 K for 24 hours, revealing the $^4A_2 \rightarrow {}^4T_1$, $^4T_2$ bands [9]. The 22 200 cm^{-1} band is thought to be due to colour centres which are common in lanthanum-based crystals. The similarity of the absorption spectrum of LGGO suggests the same cause.

The four gallogermanate crystals exhibit broad-band photoluminescence with peaks between 10 000 and 11 000 cm^{-1} when excited in either of their broad absorption bands (figure 1). An excitation spectrum of the Cr^{3+}:LGGO broad-band luminescence reveals an absorption band that peaks at 15 100 cm^{-1}. The CGGO, SGGO and LGS luminescence spectra also have sharp R lines in the region of 14 400 cm^{-1}. The R lines in LGS are very much weaker than the broad band and too weak to be identifiable in the spectra shown in figure 1.

Broad luminescence bands are the signature of Cr^{3+} ions in weak-field sites where the $^4T_2$ level is lower in energy than the ^2E state. Sharp R lines characterize transitions between the ^2E excited state and $^4A_2$ ground state on Cr^{3+} ions in strong-crystal-field sites. Such definitions should be treated casually, however, as site-to-site differences in the strength of the electron–phonon coupling energy influence the relative ordering of the states after vibronic relaxation. The implications of this have been discussed in general by Bartram *et al* [10] and demonstrated experimentally by the present authors [1]. For both broad-band and R-line fluorescence to occur at low temperature in SGGO, CGGO and LGS suggests either that both strong- and weak-field sites are present or that there is a single site with intermediate crystal-field strength for Cr^{3+} in which ^2E and $^4T_2$ levels are almost degenerate. The earlier high-resolution spectroscopic studies and electron spin-resonance (ESR) studies confirm that there are two distinct Cr^{3+} centres in CGGO and SGGO [1, 5, 11]. In LGS, the intensity of the R line is so small that it is likely to represent the tail of a distribution of crystal fields or electron–phonon coupling strengths which just spans the $^2E \rightarrow {}^4T_2$

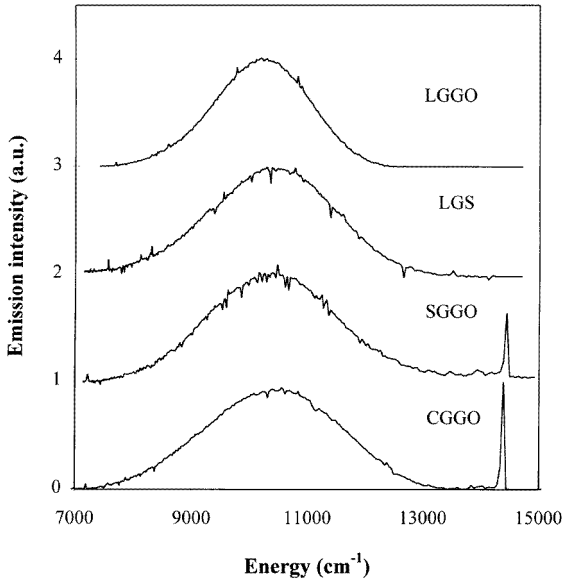

Figure 1. Fluorescence spectra of Cr^{3+} in the indicated hosts at 14 K excited by the multiline visible output of an argon-ion laser.

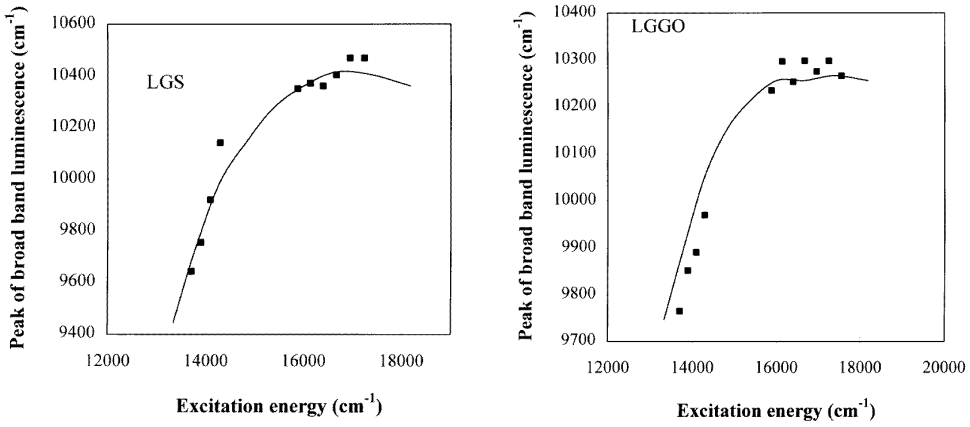

Figure 2. The dependence of the $^4T_2 \rightarrow {}^4A_2$ broad-band fluorescence peak on the excitation wavelength (symbols) of Cr^{3+} in the hosts indicated. The line represents a fit to the data as described in the text.

crossover region.

The ratio of the lifetime of the R line to that of the broad band in LGS is 10:1 ($\sim$100 μs:10 μs) whereas in SGGO and CGGO the ratios are 70:1 and 50:1 respectively [1]. As discussed previously [12, 13] the R line and broad band have equal lifetimes for a single intermediate-field site. The large difference in the lifetimes of the R lines and broad bands in Cr^{3+}:CGGO and Cr^{3+}:SGGO is consistent with two site distributions, whereas the much smaller ratio in LGS suggests a single site distribution just exceeding the crossover energy.

3.2. Inhomogeneous broadening of the $^4A_2 \leftrightarrow {}^4T_2$ transitions

In Cr^{3+}:CGGO and Cr^{3+}:SGGO the shift of the peak of the $^4T_2 \rightarrow {}^4A_2$ band with excitation energy was not linear, the shift decreasing strongly at higher energies [1]. This behaviour is also observed for LGGO and LGS (see figure 2). A slight narrowing of the luminescence band is also observed with increasing excitation energy. The inhomogeneously broadened absorption band is composed of overlapping bands from inequivalent sites, each having slightly different emission bands. As the excitation energy is changed the relative intensities of the emission spectrum are also altered, causing the observed shifts of the peak energy and variations in the width of the luminescence band.

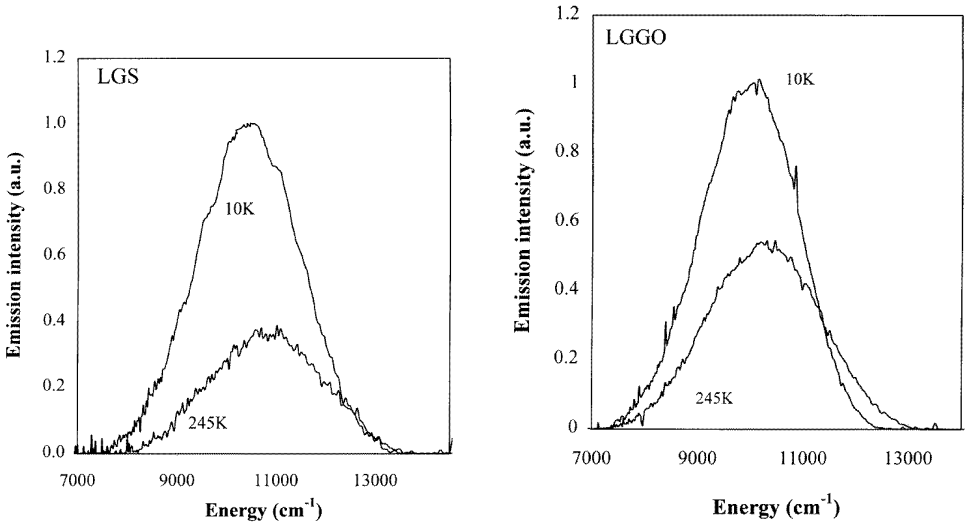

Figure 3. A comparison of $^4T_2 \rightarrow {}^4A_2$ broad-band fluorescence spectrum at 10 K and 245 K of Cr^{3+} in the hosts indicated.

Normalized luminescence spectra at 10 K and 245 K for LGGO and LGS are shown in figure 3. As for CGGO and SGGO, non-radiative decay appears to affect the low-energy side of the band more than the high-energy side, causing an apparent blue-shift of the peak of the luminescence band at 245 K. The luminescence intensities in LGS and LGGO are somewhat less affected by thermal quenching processes than in CGGO and SGGO with around 40% of the emission intensity surviving at room temperature and a blue-shift being observed that is correspondingly smaller than in SGGO or CGGO. In Cr^{3+}-doped materials, the peak of the broad luminescence band is expected to red-shift as the temperature increases because of the effect of thermal lattice expansion which reduces the crystal-field strength around the Cr^{3+} ions, lowering the energy of the $^4T_2$ electronic manifold [14]. For a single site, non-radiative decay would affect all parts of the luminescence band equally. A blue-shift is then further evidence that a multitude of sites contribute to the $^4A_2 \leftrightarrow {}^4T_2$ band, each characterized by slightly different non-radiative decay rates. The same effect has been observed in Cr^{3+}- and Mn^{2+}-doped glasses [4, 15]. In the present analysis the approach taken to characterize the inhomogeneous broadening of the band will be to model a distribution of sites (considering separate distributions of $S\overline{\hbar\omega}$ and $10Dq$) which allows the low-temperature lineshape to be reproduced at all experimental excitation wavelengths. Non-radiative effects will be considered more fully in a subsequent publication.

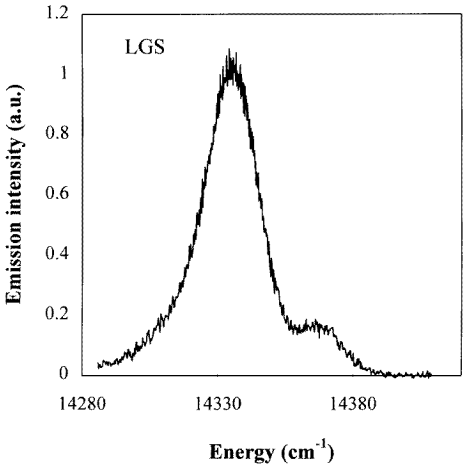

Figure 4. The R-line fluorescence at 14 K from Cr^{3+}:LGS.

3.3. Inhomogeneous broadening of the R lines

Cr^{3+}-doped LGS emits R lines as well as the broad $^4T_2 \rightarrow {}^4A_2$ bands as is the case for Cr^{3+}-doped CGGO and SGGO [1, 5]. However, for CGGO and SGGO the R linewidths are large, being greater than 50 cm^{-1}. Part of the width of these R lines is due to overlap between the R_1 and R_2 lines, the splitting being caused by the combination of spin–orbit interaction and trigonal, even-parity distortions of the CrO_6^{9-} octahedron. In LGS (figure 4) there are narrower, resolved R_1 and R_2 lines, the relative intensities of which follow a Boltzmann relationship as a function of temperature.

The mechanisms of inhomogeneous broadening of the R lines in the gallogermanates have been probed using FLN. Detailed results have already been presented for CGGO and SGGO [1], which are ideal candidates given that the R lines are quite intense, being comparable to the peak intensity of the $^4T_2 \rightarrow {}^4A_2$ band (figure 1). The R lines in LGS are much weaker. Representative FLN spectra for LGS and SGGO are compared in figure 5. For LGS, resonant FLN spectra could not be obtained because of the low intensity of the R line (and its short decay time).

In contrast, Cr^{3+}:LGGO emits only in the broad $^4T_2 \rightarrow {}^4A_2$ band and it is concluded that the LGGO crystal provides only a single distribution of weak-field sites.

Table 2. Peaks and widths of absorption and luminescence bands in gallogermanates (cm^{-1}). Absorption was measured at 77 K. Luminescence was excited at 16 100 cm^{-1} and measured at 10 K.

Crystal	FWHM ($^4A_2 \rightarrow {}^4T_2$)	FWHM ($^4T_2 \rightarrow {}^4A_2$)	Peak ($^4A_2 \rightarrow {}^4T_2$)	Peak ($^4T_2 \rightarrow {}^4A_2$)
SGGO	2300	2300	17 060	10 400
CGGO	2380	2400	16 130	10 530
LGS	2470	2510	15 380	10 400
LGGO	—	2000	15 100	10 210

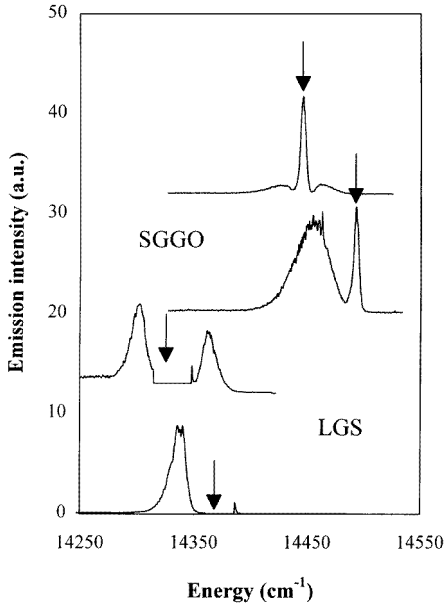

Figure 5. FLN spectra excited in the middle and in the high-energy wing of the R lines for Cr^{3+}:SGGO and Cr^{3+}:LGS. The arrows indicate the excitation energy. For SGGO, time resolution allowed resonant spectra to be taken, but for LGS the much reduced fluorescence intensity prevented this. The laser was therefore turned off as the monochromator scanned close to the excitation wavelength and this range is indicated by the very flat parts of the spectra centred on the arrows.

4. Theoretical analysis

A statistical model has been developed to model the spectroscopic data obtained from the R-line FLN spectra of strong-field Cr^{3+} sites and an adiabatic model of the spin–orbit and electron–phonon coupling interactions has been used to model the broad-band absorption and emission spectra of the weak-field Cr^{3+} sites [1]. These have been applied to CGGO and SGGO [1], $CaYAlO_4$ [16] and $LiNbO_3$ [17]. Since these models are fully described elsewhere [1], only the results and broad outline of the analyses are presented here. The primary purpose of this paper is to compare and contrast the behaviour of Cr^{3+}-doped LGGO and LGS with the isomorphic CGGO and SGGO.

4.1. Distribution of weak-field sites

The most obvious experimental evidence that the broad-band $^4A_2 \leftrightarrow {}^4T_2$ absorption and luminescence spectra are inhomogeneously broadened comes from the shift in the peak of the luminescence band with excitation energy (figure 2) and the different widths of the bands (table 2). The model developed in [1] shows that if the only consequence of disorder is a broad distribution in the value of the octahedral splitting, $10Dq$, then the emission band excited by monochromatic radiation is narrower than the width of the corresponding absorption band. However, in crystals with the gallogermanate structure, the widths of the absorption bands are less than or equal to the widths of the laser-excited emission bands. Site-to-site variations in the Huang–Rhys factor, S, are required to explain this observation.

This creates a distribution of the minima of the $^4T_2$ potential energy curves, E_i. The effect is that the energy $E_i + S_i\bar{h}\omega$, which for a Pekarian lineshape corresponds to the peak of the absorption band, is almost the same for each site whereas the energy $E_i - S_i\bar{h}\omega$ at the peak of the luminescence band varies at around twice the rate of E_i [1] thus satisfying the requirement of a narrow distribution in Dq and a broad distribution in the emission.

The luminescence lineshapes are calculated using the adiabatic model [18] in which the vibronic overlap integrals of transitions are evaluated using computer simulation routines. The Huang–Rhys parameter is assumed to change linearly with E_i such that

$$S_i\bar{h}\omega = S_0\bar{h}\omega - K(E_i - E_0) \tag{1}$$

where E_0 and S_0 are the most probable values of the minimum energy of the $^4T_2$ manifold and the Huang–Rhys parameter, respectively, each variable being assumed to have a Gaussian distribution of values.

The standard deviations of the absorption (σ_a) and luminescence (σ_e) bands are defined as

$$\sigma_a = |(1 - K)|\sigma_\Theta \qquad \sigma_e = (1 + K)\sigma_\Theta \tag{2}$$

where σ_Θ is the standard deviation of the distribution of the energies of the minima of the $^4T_2$ manifold. The parameter K to an extent describes the relative contributions of the variation of the octahedral crystal-field strength and variation in the electron–lattice coupling energy. For $K = 0$, all variations in the band-shapes of the multisite system are due to variation in the octahedral crystal field—that is, S_i is constant. For $K = 1$, only the distribution of the Huang–Rhys parameter contributes to the variation in band-shapes, so $10Dq$ is constant. For all other values of K, variations in both $10Dq$ and S contribute to the formation of the lineshape of the inhomogeneously broadened spectra. It follows from equation (2) that the standard deviation of the Huang–Rhys parameter is

$$\sigma_s = K\sigma_\Theta \tag{3}$$

where the absorption and emission band-shapes are defined by

$$\begin{aligned}\Theta_a(E_i, \sigma_a, \sigma_i) &= \Theta_a(E_i + S_i\bar{h}\omega, \sigma_a)\\ \Theta_e(E_i, \sigma_e, \sigma_i) &= \Theta_e(E_i - S_i\bar{h}\omega, \sigma_e)\end{aligned} \tag{4}$$

where Θ_a describes the contribution of the octahedral crystal field to the system energy.

Table 3. Parameters for $^4T_2 \rightarrow {}^4A_2$ luminescence model. The unit of energy is cm^{-1}.

	SGGO	CGGO	LGS	LGGO
Mean electron lattice coupling energy ($S\bar{h}\omega_0$)	3700	3200	3150	2900
Standard deviation of $S\bar{h}\omega$	320	330	312	280
Mean $^4T_2 - {}^2E$ energy	−900	−1400	−1300	−1650
Standard deviation of $^4T_2 - {}^2E$ energy	250	500	390	350
K	1.3	0.65	0.8	0.8

The selective excitation spectra of this band allow estimates of the model parameters to be obtained by calculating the emission lineshapes for each excitation wavelength, leaving the most probable electron–lattice interaction energy and minimum $^4T_2$ levels and their standard deviations as free parameters. The maximum of the absorption band is assumed to

be the peak of the Θ_a distribution. The best fitting parameters for the model were obtained and are listed in table 3.

For CGGO a value of $K = 0.65$ implies that a significant distribution of $10Dq$ in conjunction with a distribution of Huang–Rhys factors is required to explain the observed spectra whereas in SGGO, where $K = 1.3$, the inhomogeneous broadening is caused by a relatively small contribution from the distribution of $10Dq$. The values of K for LGS and LGGO at 0.8 are even closer to unity, from which it is inferred that the disorder in these crystals is dominated by the distribution of electron–lattice coupling. The increased coupling must be due to modes other than the breathing mode, that is to modes that change the symmetry of the system.

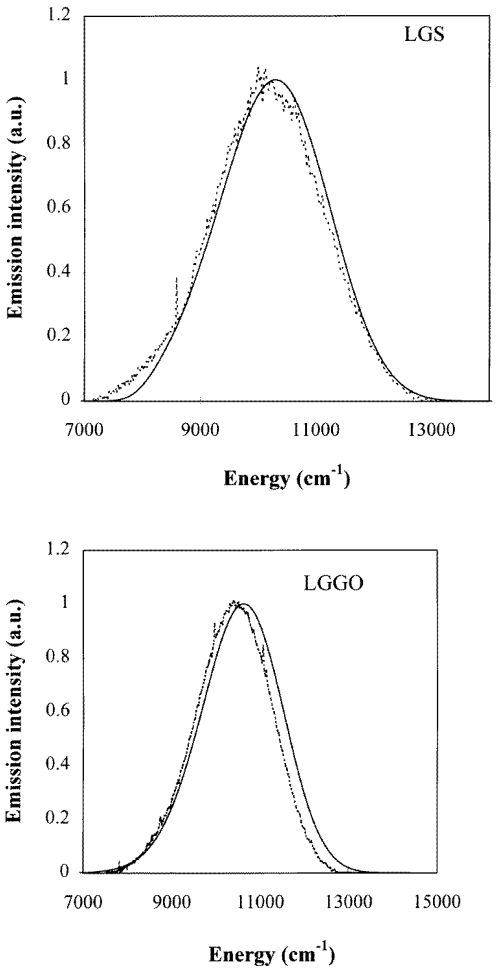

Figure 6. Simulated (solid) and experimental (dashed) fluorescence lineshapes for the $^4T_2 \rightarrow {}^4A_2$ transition of Cr^{3+} in the hosts indicated.

The peaks of the experimental spectra for different excitation wavelengths and the simulated dependence are shown in figure 2 and are in good agreement for all wavelengths considered. Luminescence spectra simulated by assuming a Pekarian lineshape for excitation at 16 700 cm^{-1} for LGS and LGGO are compared to actual spectra in figure 6 where only

the weak-field sites have been considered. In order to simulate these spectra from the model parameters listed in table 3 it was assumed that sites characterized by the lowest energy of the $^4T_2$ minima do not contribute to the luminescence. It is assumed that non-radiative processes dominate the decay for the strongly distorted sites that have the lowest values of E_i. A cut-off for sites that are considered to decay radiatively and non-radiatively is applied at a value that is half-way between E_0 and the lowest value of E_i. These sites contain about 10% of the total population of Cr^{3+} ions. The cut-off is chosen to give the best fit to the data but the fit is still imperfect. The discrepancy between the model and experimental data is attributed to the unphysical nature of this sudden cut-off. In fact, the lower-energy sites will decay through competing radiative and non-radiative processes that complicate the analysis.

The evidence provided by absorption and fluorescence band-shapes, the shift of the fluorescence peak with excitation energy and the shift of the fluorescence peak with temperature all indicate that the principal effect of the substitutional disorder in the gallogermanate lattice is to cause a distribution in the electron–phonon coupling energies rather than to influence the average crystal field. This is interpreted as being due to the effect of the variation in the non-octahedral crystal field dominating the effect of the variation in the octahedral crystal field. The proximity of the substitutionally disordered site to the optically active ion does not appear to be important, though the only crystals in which the distribution of non-octahedral crystal-field components has been shown to dominate the broadening of the optical transitions are those in which substantial substitutional disorder is present.

4.2. Distribution of strong-field sites

In developing a model to describe the inhomogeneous broadening of the R lines the starting point is crystal-field theory which predicts that the energy of the ^2E state, or the mean energy of a split ^2E state, weakly depends upon the strength of the octahedral crystal field. The crystal field can be separated into two components; the octahedral component which can influence the centre energy of the R line and the non-octahedral component which is involved in the splitting [19]. Only distortions of even parity are of significance in discussing centre energies or splittings of the R lines. Uniaxial stress experiments in ruby have shown that the R-line splitting increases as the applied stress is increased (i.e. the trigonal distortion is enhanced) but the barycentre of the transitions remains fixed: the trigonal distortion causes the lines to split equally about a mean energy [20].

It is convenient to discuss two independent distributions of the crystal field that take into account the octahedral and the non-octahedral components, and such a model has been developed and fully described elsewhere [1]. The model considers a Gaussian distribution of splittings, Θ_Δ, with a standard deviation σ_Δ caused by the non-octahedral contribution to the crystal field and a Gaussian distribution of centre energies, Θ_E, with a standard deviation of σ_E caused by the octahedral contribution. It has been shown for a number of substitutionally disordered crystals that the contribution of the non-octahedral crystal field dominates the inhomogeneous broadening of the R lines [1, 16].

The parameters that describe the splitting may be obtained through an analysis of the non-resonant fluorescence spectra and FLN data. If the transition probability is the same from the ground state to each ^2E state and for each site, then the density of states is equivalent to the absorption lineshape. As electron–phonon coupling is very weak in the ^2E state the absorption lineshape is equivalent to the purely electronic part of the non-resonant fluorescence spectrum. For the model as developed, the upper and lower ^2E densities of

Table 4. Distributions of inhomogeneous broadening of R lines in CGGO, SGGO and LGS (cm^{-1}). (1) σ_E calculated from the non-resonant FLN linewidth. (2) σ_E calculated from the slope of Δ_{eff} against FLN excitation energy.

	CGGO	SGGO	LGS
σ_R	19.4	20.7	14.1
$\sigma_E^{(1)}$	17.5	17.3	13.8
σ_Δ	25.0	18.0	6.0
$\sigma_E^{(2)}$	16.4	17.2	14.0
Δ_0	22	30	31
E_0	14 399	14 455	14 360

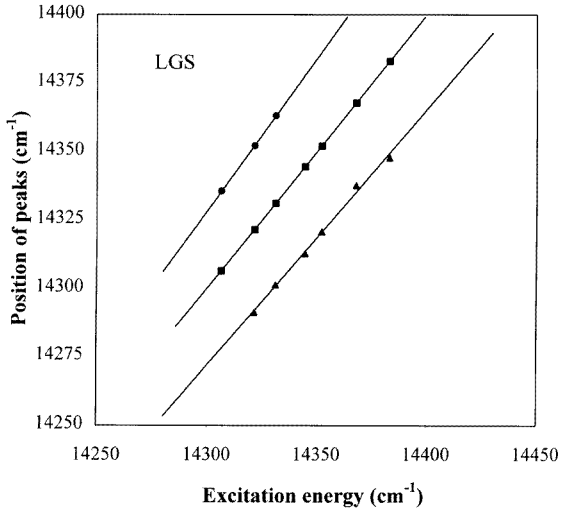

Figure 7. Positions of features in FLN spectra for Cr^{3+}:LGS. Squares indicate resonant fluorescence, circles represent fluorescence from the R_2 line excited in the R_1 line and triangles fluorescence from the R_1 line excited in the R_2 line.

states have the same shape but are centred around the energies $E_0 + \Delta_0/2$ and $E_0 - \Delta_0/2$. In such a case, both densities of states have the same standard deviation, σ_R, which is given by

$$\sigma_R = \sqrt{\sigma_E^2 + \frac{1}{4}\sigma_\Delta^2}. \tag{5}$$

The standard deviation of the non-resonant emission red- or blue-shifted from the resonant line is given by

$$\sigma_{\Delta_{eff}} = 2\sqrt{\frac{\sigma_E^2\sigma_\Delta^2}{4\sigma_E^2 + \sigma_\Delta^2}}. \tag{6}$$

The standard deviation of the density of states, σ_R, is obtained from a Gaussian fit to the non-resonantly excited, inhomogeneously broadened R_1 emission line and $\sigma_{\Delta_{eff}}$ may be obtained from a Gaussian fit to the non-resonant R_1 line excited in the high-energy wing of the R_2 line. From these parameters, the standard deviations of the centre energy and splitting distributions may be calculated from equations (5) and (6). The most probable centre energy is the excitation energy for which the blue- and red-shifted non-resonant emission features have the smallest energy separation from the resonant line. The most probable splitting is then obtained from the peak energy of the inhomogeneously broadened R line. This process

has already been completed for CGGO and SGGO [1] and the calculated parameters can be compared with the data for LGS (recall that LGGO has no detectable R-line fluorescence) obtained in this study in table 4.

The positions of the peaks of the resonant and non-resonant lines from the FLN experiments are plotted against excitation energy in figure 7 and this can be used to make a second estimation of the parameter σ_Δ [1]. The separation of resonant and non-resonant emission peaks is referred to as the effective splitting, Δ_{eff}:

$$\Delta_{eff} = \pm 2(E - E_0)Q_\Delta + \Delta_0 Q_E \tag{7}$$

where the parameters Q_E and Q_Δ are given by the expressions:

$$Q_E = \frac{4\sigma_E^2}{4\sigma_E^2 + \sigma_\Delta^2} \qquad \text{and} \qquad Q_\Delta = \frac{\sigma_\Delta^2}{\sigma_\Delta^2 + 4\sigma_E^2}. \tag{8}$$

Thus the effective splitting is linearly dependent on the excitation energy. The slope of the line is Q_Δ and is zero when there is no correlation between Δ_{eff} and the excitation energy, or equivalently when the width of the splitting distribution is small in comparison to the width of the centre energy distribution. A large value of the slope will indicate a significant contribution to the inhomogeneous broadening from the variation in splitting. Plotting the effective splitting against excitation energy allows the value of Q_Δ to be obtained from the slope, which permits an estimate of σ_E to be derived independently of the width of the non-resonant emission, $\sigma_{\Delta_{eff}}$. Figure 7 shows that the separation between resonant and non-resonant features is almost independent of wavelength, so Q_Δ is small for LGS. The value of σ_E for LGS is consequently also small as determined from the linewidth of the non-resonant FLN features. The values for all of the gallogermanates as calculated from the slope are listed in table 4 and are close to the values calculated independently, suggesting that the model is reliable.

As discussed previously [1], in SGGO and CGGO the magnitudes of the standard deviations of the splitting distributions are larger than the standard deviations of the centre energies of the transitions, inferring that to a large extent the R lines in these materials are inhomogeneously broadened by a distribution of low-symmetry fields. In contrast, the standard deviation of the splitting distribution of LGS is narrower than the standard deviation of the centre energy, resulting in the near independence of the effective splitting on excitation energy. In this material, the contribution to the inhomogeneous broadening by low-symmetry fields is small. Despite the crystal structures of the two materials being very similar and both lattices being substitutionally disordered there is a significant difference in the mechanism that determines the broadening of the R lines. It is important to note, however, that the broadening of the $^4T_2 \rightarrow {}^4A_2$ band was shown above to be dominated by the non-octahedral component of the crystal field for all four crystal hosts investigated.

There is a simple explanation for the apparent differences in the broadening of the different spectral features in different gallogermanate hosts. As is evident from lifetime data discussed above and ESR results [11], CGGO and SGGO contain two different sets of centres, each of which has a separate set of parameters describing its crystal-field distributions, whereas LGS and LGGO appear to have a single distribution of sites. Under these circumstances, the R line in LGS represents only one extreme of the distribution. The bulk of the sites contribute to the $^4T_2 \rightarrow {}^4A_2$ fluorescence and the broadening of this band has been shown to be dominated by non-octahedral components of the crystal field. Those sites that contribute to the R line are therefore those at the extreme of the distribution of the non-octahedral crystal field. The variation of the non-octahedral contribution component of the crystal field across the R line is therefore expected to be small. The variation of the

octahedral crystal field may be larger, as the domination of the non-octahedral crystal field tends to spread the distribution of octahedral crystal fields throughout the overall distribution. This is observed. Table 4 shows that σ_Δ is considerably reduced in LGS whereas σ_E is only slightly less than in CGGO and SGGO.

The broadening of the R lines in LGS has therefore been shown to be consistent with the broadening mechanisms determined for the optical transitions of Cr^{3+} in the gallogermanate family as a whole. The apparent lack of broadening due to the distribution of non-octahedral crystal-field components is simply due to the fact that the R lines represent the wings of a much larger distribution.

5. Conclusion

It has been shown that Cr^{3+} ions occupy trigonally distorted octahedral sites in gallogermanate hosts. For the case of SGGO and CGGO, two distributions of sites are present, giving rise to separate sharp-line and broad-band emission spectra, whereas for LGGO and LGS, one site distribution is adequate to describe the optical spectra. The broadening of all distributions has been shown to be dominated by the contribution of the non-octahedral crystal field.

The question of why there should be two distributions of sites in SGGO and CGGO resulting in the concurrence of R-line and broad-band luminescence is an important one. It seems likely that the proximity of the substitutionally disordered sites to the optically active ion is important. As noted in table 1, the disorder affects the nearest cation shell (3f site) and the 1a octahedra in CGGO and SGGO, but is restricted to the 2d tetrahedra in LGS. ESR studies show that the two sets of sites in CGGO and SGGO can be differentiated by the presence or absence of a further, orthorhombic distortion to the trigonally distorted octahedral site [11]. The trigonally symmetric sites appear to be less populous in the ESR spectra and have therefore been attributed to the strong-field sites. The likely explanation for the difference between the two sets of sites is the arrangement of ions in the 3f nearest-cation-neighbour shell. To maintain trigonal symmetry, the occupation of the six nearest 3f sites must consist of layers, perpendicular to the *c*-axis, of three like ions. The orthorhombically distorted sites may have any other irregular arrangement of Ga^{3+} and Ge^{4+} ions about the Cr^{3+} ion. Clearly, such possibilities do not exist in LGGO and LGS where the 3f sites are always occupied by Ga^{3+} ions. The conclusion must be that close-range disorder is required to produce separate distributions of sites, but that longer-range disorder is still sufficient to cause the broadening of each distribution to be dominated by the variation in non-octahedral crystal-field contributions.

Acknowledgments

The authors are grateful to the EPSRC and MOD for their joint award of research grants GR/F/54009 and GR/F/54105. One of us (KH) is indebted to the Nuffield Foundation for partial support of his work. PIM wishes to thank the EPSRC and MOD for the award of a CASE studentship. Travel grants to support this collaborative project were given by a joint British Council and Komitet Badan Naukowych award. All samples were purchased from the Crystal Laser Physics Laboratory in Moscow.

References

[1] Grinberg M, Macfarlane P I, Henderson B and Holliday K 1995 *Phys. Rev.* B **52** 3917
[2] Bergin F, Donegan J F, Glynn T J and Imbusch G F 1986 *J. Lumin.* **34** 307
[3] Ogihara C, Gao Y, O'Donnell K P, Henderson B and Yamaga M 1992 *J. Phys.: Condens. Matter* **4** 4853
[4] Yamaga M, Henderson B, O'Donnell K P and Gao Y 1991 *Phys. Rev.* B **44** 652
[5] Macfarlane P I, Han T P J, Henderson B and Kaminskii A A 1994 *Opt. Mater.* **3** 15
[6] Belokoneva E L, Butashin A V, Simonov M A, Mill B V and Belov N V 1980 *Dokl. Akad. Nauk SSR* **5** 255
[7] Kaminskii A A, Belokoneva E L, Mill B V, Pisarevski Y V, Sarkisov S E, Silvestrova I M, Butashin A V and Khodzhabagyan I M 1984 *Phys. Status Solidi* **86** 345
[8] Kaminskii A A, Butashin A V, Demidovich A A, Koptev V G, Mill B V and Shkadarevich A P 1989 *Phys. Status Solidi* a **112** 197
[9] Lai S T, Chai B H T, Long M and Shiria M D 1988 *IEEE J. Quantum Electron.* **9** 24
[10] Bartram R H, Charpie J C, Andrews L C and Lempicki A 1986 *Phys. Rev.* B **34** 2741
[11] Yamaga M, Takeuchi H, Yosida M, Henderson B, Macfarlane P I and Holliday K, in preparation
[12] Grinberg M, Brenier A, Boulon G, Pedrini C and Madej C 1993 *J. Lumin.* **55** 303
[13] Yamaga M, O'Donnell K P, Gao Y and Henderson B 1990 *App. Phys.* B **51** 132
[14] Henderson B, Marshall A, Yamaga M, O'Donnell K P and Cockayne B 1988 *J. Phys. C: Solid State Phys.* **21** 6187
[15] Szörényi T, L. Szöllõsy and Szanka K 1976 *Phys. Chem. Glasses* **17** 104
[16] Yamaga M, Macfarlane P I, Holliday K, Henderson B, Kodama N and Inoue Y 1996 *J. Phys.: Condens. Matter* **8** at press
[17] Macfarlane P I, Holliday K and Henderson B 1996 *Chem. Phys. Lett.* at press
[18] Grinberg M 1993 *J. Lumin.* **54** 369
[19] Macfarlane R M 1967 *J. Chem. Phys.* **47** 2066
[20] Sharma S M and Gupta Y M 1989 *Phys. Rev.* B **40** 3329